

Verwey transition in magnetite: Mean-field solution of the three-band model

S. K. Mishra, Z. Zhang,^{a)} and S. Satpathy

Department of Physics and Astronomy, University of Missouri, Columbia, Missouri 65211

The nature of the Verwey transition in magnetite (Fe_3O_4) within a three-band spinless model Hamiltonian is examined. These bands, which arise from the minority-spin t_{2g} orbitals on the $\text{Fe}(B)$ sublattice, are occupied by half an electron per $\text{Fe}(B)$ atom. The Verwey order–disorder transition is studied as a function of the ratio of the intersite Coulomb repulsion U_1 and the bandwidth W . It is found that the electrons are ordered beyond the critical value of $U_1/W \approx 0.25$ in essential agreement with the results of the one-band Cullen–Callen model. For larger values of U_1/W , a Verwey-like order is exhibited where the electrons occupy alternate (001) planes. The model predicts a transition from the metallic to the semiconducting state with the band gap increasing linearly with U_1 beyond the transition point.

I. INTRODUCTION

The Verwey transition in magnetite^{1–3} is a well-known metal–insulator transition characterized by a decrease of two orders of magnitude in conductivity as temperature is decreased below the Verwey temperature of $T_v \sim 120$ K. The transition is accompanied by an order–disorder transition, where in the simplest ionic picture, Fe^{2+} and Fe^{3+} ions order on the B sublattice of the spinel structure, interacting via Coulomb forces. Examining this picture quite early on, Anderson⁴ pointed out the remarkable property of the spinel B sublattice that the short-range part of the Coulomb interaction is minimized by $\sim (3/2)^{N/2}$ different configurations of the ions where N is the number of sites on the B sublattice. The long-range part of the Coulomb interaction, on the other hand, is minimized only by a few of these configurations. The Verwey transition may therefore be interpreted as a loss of long-range order (LRO) above T_v with no abrupt change in the short-range order (SRO). This interpretation is consistent with the entropy change at the Verwey transition obtained from specific heat measurements.

This ionic picture, while providing a reasonable description of the order–disorder transition, does not provide any quantitative description of the transition from metal to insulator. Issues unaddressed include questions such as: What are the charge carriers in magnetite? Is the conductivity via motion of ions or does one have to think of itinerant electrons? In fact, subsequent to Anderson's work, a number of models have been proposed to describe the mechanism of electrical conduction and simultaneously the order–disorder transition. These include the itinerant one-band electron model of Cullen and Callen,⁵ and the molecular polaron or bipolaron pictures of Yamada and Chakraverty,⁶ etc.

The itinerant electron model of Cullen and Callen describes the Verwey transition in terms of motion of electrons on the B sublattice. The Hamiltonian consists of a nearest-neighbor hopping integral t and the intersite Coulomb interaction U_1 between nearest neighbors. In a seminal work,⁵ Cullen and Callen studied this model and in fact found an order–disorder transition below a critical value of $U_1/t \sim 2.2$. However, there was no justification for the origin of such a

model and, since there was no reliable estimate for U_1/t until our recent work,⁷ the applicability of the Cullen–Callen model to magnetite remained unclear.

Recently we have examined the electronic structure of magnetite using density-functional methods with the local spin-density approximation (LSDA).⁷ Based on this work, we have obtained a three-band electronic Hamiltonian for the motion of electrons on the B sublattice of magnetite. In this article, we discuss the results of a mean-field solution of the three-band model. We find that both (a) the order–disorder transition and (b) the metal–insulator transition can be described within the three-band model.

II. THE MODEL HAMILTONIAN

The crystal structure of magnetite consists of three sublattices, viz., the oxygen sublattice and the $\text{Fe}(A)$ and the $\text{Fe}(B)$ sublattices. The magnetic moments within each Fe sublattice are aligned in the same direction, while the two sublattices are aligned antiferromagnetically. Since there are twice as many atoms on the B sublattice as on A , there is a net magnetic moment with a magnitude of $4.1 \mu_B$ per Fe_3O_4 formula unit.

In our earlier work,⁷ we have calculated the density-functional spin-polarized electronic structure of magnetite, which is schematically shown in Fig. 1. As seen from the figure, the majority-spin bands are semiconducting, while the minority-spin bands are metallic, a picture also obtained by Yanase and Siratori from independent calculations.⁸ The presence of only the minority-spin electrons at the Fermi energy is consistent with the spin-polarized photoemission experiments of Alvarado *et al.*⁹

The t_{2g} orbitals of the $\text{Fe}(B)$ atoms form the electron bands at the Fermi energy E_f with the t_{2g} bands occupied by half an electron per $\text{Fe}(B)$ atom. The electron count is such that the presence of these “extra” electrons makes the valency of half the B site atoms Fe^{+2} and the other half B site atoms have the valency of Fe^{+3} . The picture that emerges then is that the “extra” electrons move on the background of Fe^{+3} atoms on the B sublattice in agreement with the traditional view of charge transport in magnetite.⁴

The electronic structure provides justification for the conventional picture of conduction via $\text{Fe}(B)$ electrons moving on the B sublattice. However, unlike the one-band pic-

^{a)}Present address: Department of Physics, North Carolina State University, Raleigh, NC 27695.

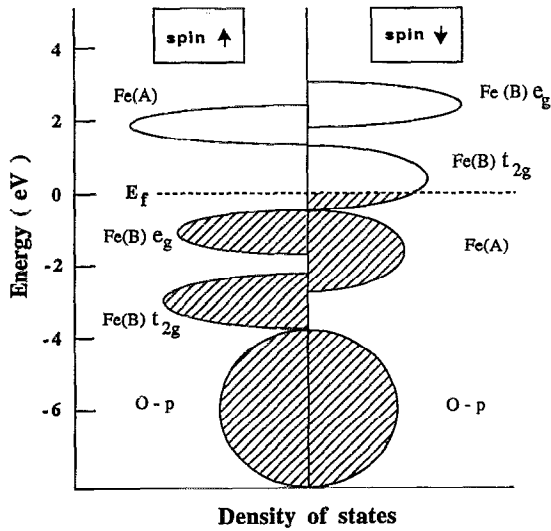


FIG. 1. Schematic picture of the electronic structure in magnetite as obtained from the density-functional band calculation (Ref. 7). The minority spin t_{2g} electrons on the Fe(B) sublattice play the key role in charge transport.

ture of Cullen and Callen, we now have the three t_{2g} bands (xy , yz , and zx), which leads to a three-band electron model on the B sublattice

$$H = \sum_{\langle ij \rangle} \sum_{\mu, \nu=1}^3 t_{\mu, \nu} a_{i\mu}^+ a_{j\nu} + \sum_{ij} \sum_{\mu, \nu=1}^3 U_{i\mu, j\nu} n_{i\mu} n_{j\nu}. \quad (1)$$

Here $a_{i\mu}^+$ ($a_{i\mu}$) are the creation (annihilation) operators of the electron on the B sublattice with i , μ being the site and orbital indices (xy, yz, zx), respectively, $n_{i\mu}$ is the corresponding number operator, and $\langle ij \rangle$ denotes summation over nearest neighbors (NN). The Hamiltonian (1) consists of a tight-binding NN hopping term (the band-structure term) plus the Coulomb interaction term.

The values of the electronic parameters in the Hamiltonian (1), calculated from “constrained” density-functional methods,⁷ have the following values for magnetite: (a) the hopping integrals $t_{dd\sigma} = -0.41$ eV, $t_{dd\pi} = 0.05$ eV, and $t_{dd\delta} = 0.12$ eV, resulting in an average $t \approx -0.13$ eV and a bandwidth of $W = 1.55$ eV and (b) the Coulomb parameters $U_0 = 4.1 \pm 0.5$ eV, $U_1 = 0.3 - 0.4$ eV, and $U_2 \approx 0.05 - 0.1$ eV. Here the on-site Coulomb repulsion is denoted by U_0 and the first and the second NN Coulomb terms are denoted by U_1 and U_2 , respectively. Since U_0 is much larger than U_1 and $t_{\mu\nu}$, double site occupancy is prevented in view of the fact that there are half as many electrons as the B sites. Although a small value of U_2 is necessary to stabilize¹⁰ the experimentally observed “Mizoguchi structure” at low temperatures,¹¹ a structure where the unit cell is doubled, U_2 is an unimportant parameter for our purpose here. In our study below, we choose the values of $U_0 = 4$ eV and $U_2 = 0$, leaving thereby the only relevant parameter U_1/W in the Hamiltonian.

III. MEAN-FIELD SOLUTION

We study the Verwey transition by solving the Hamiltonian (1) in the mean-field approximation. We retain the

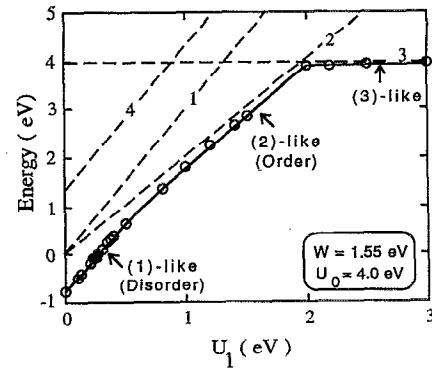


FIG. 2. Ground-state energy as a function of U_1 . The dashed curves correspond to energies in the limit of zero hopping (no kinetic energy term) for various configurations. The configurations are characterized by the mean occupation of the xy, yz, zx orbitals on the four Fe(B) atoms, viz., (1) $\{1/2, 0, 0; 1/2, 0, 0; 1/2, 0, 0; 1/2, 0, 0\}$, (2) $\{1, 0, 0; 1, 0, 0; 6 * 0\}$, (3) $\{1, 1, 0; 9 * 0\}$, and (4) $\{12 * 1/6\}$. The Coulomb energy of the four configurations are (1) $E = 3U_1$, (2) $E = 2U_1$, (3) $E = U_0$, and (4) $E = U_0/3 + 3U_1$. Even though the Coulomb energy of configuration (1) is relatively high, the large kinetic energy gain for this configuration makes it the ground state for lower values of U_1 . Configuration (2) wins beyond the transition point of $U_1 \approx 0.38$ eV because of its lower Coulomb energy.

periodicity of the spinel structure, which means the electrons can occupy any of the twelve orbitals [four Fe(B) atoms \times three orbitals/atom] in the unit cell. In the standard mean-field approximation, we have

$$n_{i\mu} n_{j\nu} \approx \langle n_{i\mu} \rangle \langle n_{j\nu} \rangle + n_{i\mu} \langle n_{j\nu} \rangle - \langle n_{i\mu} \rangle \langle n_{j\nu} \rangle. \quad (2)$$

Incorporating the first two terms in the band-structure part of Eq. (1), the total energy may then be written as a sum over the occupied one-electron eigenvalues ε_i minus the Coulomb energy

$$E = \sum_i^{\varepsilon_F} \varepsilon_i - E_{\text{Coulomb}}. \quad (3)$$

The mean electron occupations $\langle n_{i\mu} \rangle$ are calculated from the eigenfunctions of the Hamiltonian (1), which in turn depends on $\langle n_{i\mu} \rangle$. These are then determined self-consistently. The procedure is thus to diagonalize the 12×12 Hamiltonian matrix for each k point in the Brillouin zone and find the $\langle n_{i\mu} \rangle$ from the eigenvectors of the occupied states. We then go back and find the eigenvalues and eigenvectors taking these new values of $\langle n_{i\mu} \rangle$ in the Hamiltonian. The process is repeated until $\langle n_{i\mu} \rangle$ values have converged, which then corresponds to the minimum energy configuration. We performed the eigenvalue summation in the expression (3) with 216 k points in the full Brillouin zone.

The calculated ground-state energy is shown in Fig. 2 as a function of the parameter U_1 . The dashed curves refer to the energies of selected configurations without the band-structure term, i.e., in the limit of zero bandwidth. Without the band-structure term, the ordered phase, denoted by configuration (2) in Fig. 2, has the lowest energy for all values of $U_1 \leq 2$ eV. This phase has the electron configuration where two of the four sites in the unit cell have an electron each and the other two sites are empty. However, with the inclusion of

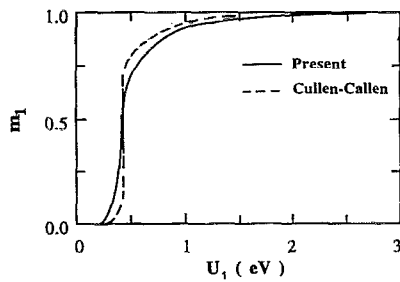


FIG. 3. The calculated Cullen–Callen order parameter m_1 as a function of the nearest-neighbor Coulomb energy U_1 .

the band-structure term, the disordered phase, viz., configuration (1), with half an electron on each site, has the lowest energy for the smaller values of U_1 . For higher values of U_1 , the Coulomb energy of configuration (1) becomes progressively larger and the ordered phase, configuration (2), wins over thereby resulting in a structural phase transition as indicated in the figure. Thus the transition is a result of the competition between the kinetic energy (band-structure energy) and the Coulomb energy.

The ordered phase is similar to the Verwey order with electrons occupying alternate (100) planes in the cubic structure. The so-called “Mizoguchi” structure,¹¹ inferred to be the structure of magnetite at low temperatures, where the unit cell has doubled compared to the cubic cell, is not reproduced in our calculation because we have restricted ourselves to the cubic unit cell of the spinel structure. To study the nature of the transition, we define the order parameters following earlier authors:⁵

$$\begin{aligned} m_1 &= (n_1 + n_2 - n_3 - n_4)/2, \\ m_2 &= (n_1 - n_2 + n_3 - n_4)/2, \\ m_3 &= (n_1 - n_2 - n_3 + n_4)/2, \end{aligned} \quad (4)$$

and

$$n = (n_1 + n_2 + n_3 + n_4) = 2.$$

Here $n_i = \sum_{\mu=1}^3 \langle n_{i\mu} \rangle$. For perfect order $m_1 = 1$, while for perfect disorder $m_1 = 0$.

The calculated order parameter m_1 as a function of the Coulomb parameter U_1 is shown in Fig. 3, where we also reproduce the results of the one-band Cullen–Callen model. There is a rather sharp transition around the value of $U_1 \approx 0.38$ eV in both the Cullen–Callen model and the present three-band model. The order parameters m_2 and m_3 are zero everywhere except the transition region corresponding to “multiple order,”⁵ an issue we have not examined yet in any detail.

We have also calculated the mean-field electronic eigenvalues (band structure). The bands are metallic until the transition point beyond which a band gap develops with the gap value increasing linearly with U_1 as shown in Fig. 4.

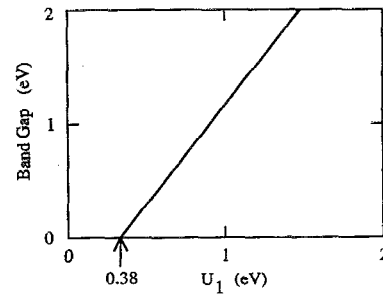


FIG. 4. Band gap as a function of the nearest-neighbor Coulomb energy U_1 . A metal–insulator transition is seen at the value of $U_1 = 0.38$ eV.

IV. CONCLUSION

In conclusion, we have studied the three-band model for the Verwey transition in magnetite in the mean-field approximation. The Verwey transition is described in terms of the order–disorder transition of the t_{2g} “extra” electrons on the B sublattice. Whether these electrons are ordered or not depends on the relative strengths of the Coulomb energy and the kinetic energy, characterized by the Coulomb parameter U_1 and bandwidth W , respectively. For lower values of the Coulomb parameter, a disordered state is favored, while a larger value results in an ordered state with the crossover taking place at the ratio $U_1/W \approx 0.25$. The ordered state in our calculation has a Verwey-like order, where alternate (001) planes on the B sublattice are occupied by the “extra” electrons. We have shown earlier¹⁰ that given the degree of freedom (larger unit cell) the kinetic energy term destabilizes the Verwey order into the experimentally observed Mizoguchi order. Finally, even though the Verwey transition occurs as temperature is changed, our present results pertain to zero temperature with the Verwey transition taking place as electronic parameters are varied. We are currently studying the Verwey transition within a finite-temperature mean-field theory. Preliminary results indicate that our model can explain the experimentally observed Verwey transition as a function of temperature.¹²

¹N. F. Mott, *Metal-Insulator Transitions* (Taylor & Francis, London, 1964).

²E. J. W. Verwey, *Z. Krist.* **91**, 65 (1935); E. J. W. Verwey and P. W. Haayman, *Physica* **8**, 979 (1941); E. J. W. Verwey, P. W. Haayman, and F. C. Romeijn, *J. Chem. Phys.* **15**, 181 (1947).

³For an overview of the Verwey transition in magnetite, see *Philos. Mag.* **42**, 327 (1980).

⁴P. W. Anderson, *Phys. Rev.* **102**, 1008 (1956).

⁵J. R. Cullen and E. R. Callen, *Phys. Rev. B* **7**, 397 (1973).

⁶Y. Yamada, *Philos. Mag. B* **42**, 377 (1980); B. K. Chakraverty, *Solid State Commun.* **15**, 1271 (1974).

⁷Z. Zhang and S. Satpathy, *Phys. Rev. B* **44**, 13 319 (1991).

⁸A. Yanase and K. Siratori, *J. Phys. Soc. Jpn.* **53**, 312 (1984).

⁹S. F. Alvarado, W. Eib, F. Meier, D. T. Pierce, K. Sattler, H. C. Siegmann, and J. P. Remeika, *Phys. Rev. Lett.* **34**, 319 (1975).

¹⁰S. K. Mishra and S. Satpathy, *Phys. Rev. B* **47**, 5564 (1993).

¹¹M. Mizoguchi, *J. Phys. Soc. Jpn.* **44**, 1512 (1978).

¹²M. Samiullah *et al.* (to be published).